DOI: 10.1002/ejic.200800413

Synthesis, X-ray Crystallography, Spectroelectrochemistry and Computational Studies on Potential Copper-Based Radiopharmaceuticals

Jason P. Holland,*[a] Peter J. Barnard,[a] David Collison,[b] Jonathan R. Dilworth,*[a] Ruth Edge,[b] Jennifer C. Green,*[a] Julia M. Heslop,[a] Eric J. L. McInnes,[b] Christoph G. Salzmann,[a] and Amber L. Thompson[c]

Keywords: Metal chelates / Radiopharmaceuticals / Density functional calculations / Hypoxia / Spectroelectrochemistry

The synthesis of metal(II) complexes of a bis(thiosemicarbazonato) ligand derived from 1,2-cyclohexanedione are reported. The compounds have been characterised by a range of techniques including reverse-phase HPLC, cyclic voltammetry, NMR, UV/Vis, IR, Raman and EPR spectroscopy. X-ray crystal structures of the proligand and two copper(II) complexes have been obtained, and the electronic structures have been analysed by using DFT calculations. DFT calculations have also been used to map the potential energy surface of a related bis(thiosemicarbazone) proligand and predict solution-phase one-electron reduction potentials of the copper(II) complex by using three polarisable continuum solvation models. Electrochemistry experiments show that the copper(II) complex undergoes quasi-reversible one-electron reduction at biologically accessible potentials and is within the range proposed for the complex to be hypoxia-selective. In addition, UV/Vis spectroelectrochemistry experiments have been used to characterise the reduced copper(I) anion, and the reaction between the anion and dioxygen has been characterised by experiments and theory. Observation of this oxidation reaction has important implications for the proposed mechanisms of hypoxia selectivity of bis(thiosemicarbazonato)copper(II) complexes. The copper-64 radiolabelled complex has been prepared in aqueous solution which demonstrates the potential of use of these complexes as medical imaging agents.

Introduction

Over the last decade, increasing clinical demand for medical imaging techniques including positron emission tomography (PET), single-photon emission computerised tomography (SPECT) and hybrid PET-computerised tomography (PET-CT) has led to widespread interest in the development of new potential imaging agents.[1–5] Recent government strategies in the United Kingdom and across Europe have also highlighted the importance of PET imaging in the diagnosis and treatment of cancer, and plans for the provision of new national facilities are well underway.[1]

Most potential radiopharmaceuticals have been developed using either technetium-99m[6] or main group radionuclides with short half-lives including iodine-131,[5,7] fluorine-18,[8] oxygen-15[9] and carbon-11.[10] However, radionuclides of metals including copper, gallium and zirconium are currently the subject of intense research due to their versatile coordination chemistry and potential applications in both imaging and radiotherapy.[3]

Tumour hypoxia is a pathological condition where tissue oxygenation is approximately <10 Torr, compared with normal levels of 20–80 Torr.[11–13] A range of copper(II) complexes of N_2S_2 tetradentate bis(thiosemicarbazonato) ligands have been characterised as antitumour agents with potential use as radiopharmaceuticals for imaging and therapy of tumour hypoxia.[2,14–16] In particular, the copper(II) complex of the biacetyl bis(4-methylthiosemicarbazaonato) ligand, [Cu^{II}ATSM], has received approval for multicentre human trials imaging cervical cancer patients.[17–19]

This paper describes the synthesis and characterisation of a new potentially hypoxia-selective bis(thiosemicarbazonato)metal(II) complexes derived from 1,2-cyclohexanedione. X-ray crystal structures of the proligand and copper(II) complex have been obtained. The copper(II) complex has also been studied using a range of techniques including cyclic voltammetry (CV), infrared (IR), Raman and electron paramagnetic resonance (EPR) spectroscopy and electronic absorption spectroelectrochemistry (UV/Vis-SEC). Density functional theory (DFT) calculations have been used to understand the electronic structure, predict

[a] Chemistry Research Laboratory, Department of Chemistry, University of Oxford,
12 Mansfield Road, Oxford, OX1 3TA, UK
E-mail: jason.holland@chem.ox.ac.uk
jon.dilworth@chem.ox.ac.uk
jennifer.green@chem.ox.ac.uk
[b] EPSRC National Service for EPR Spectroscopy, School of Chemistry, The University of Manchester,
Oxford Road, Manchester, M13 9PL, UK
[c] Chemical Crystallography, Chemistry Research Laboratory, Department of Chemistry, University of Oxford,
12 Mansfield Road, Oxford, OX1 3TA, UK
Supporting information for this article is available on the WWW under http://www.eurjic.org or from the author.

solution-phase redox potentials and, for the first time, assign the IR and Raman vibrational modes in the spectra of the copper(II) complex. In addition, the copper-64 radiolabelled complex has been prepared in aqueous solution.

Results and Discussion

Synthesis and X-ray Crystallography

Structures of the symmetrical 1,2-cyclohexanedione bis(4-methylthiosemicarbazone) [H_2HTSM (**1**)] proligand, and metal(II) complexes **2**–**6**, are shown in Scheme 1. Details of the nomenclature of acronyms used have been described elsewhere.[20] Proligand **1** was synthesised from 1,2-cyclohexanedione and 4-methylthiosemicarbazide using a similar procedure described by Mohan et al.[21] and was isolated in low yield (26%) as yellow crystals. The corresponding neutral metal(II) complexes **2**–**4** were isolated in good yields as microcrystalline powders following a procedure based on that described by Rodriguez-Argüelles et al.[22] All compounds have been fully characterised using techniques including elemental analysis, mass spectrometry, reverse-phase gradient high performance liquid chromatography (HPLC), UV/Vis spectroscopy, X-band EPR spectroscopy and CV. In addition, density functional theory (DFT) calculations have been used to investigate the electronic and vibrational structure of the proligand **1** and copper complex **2**.

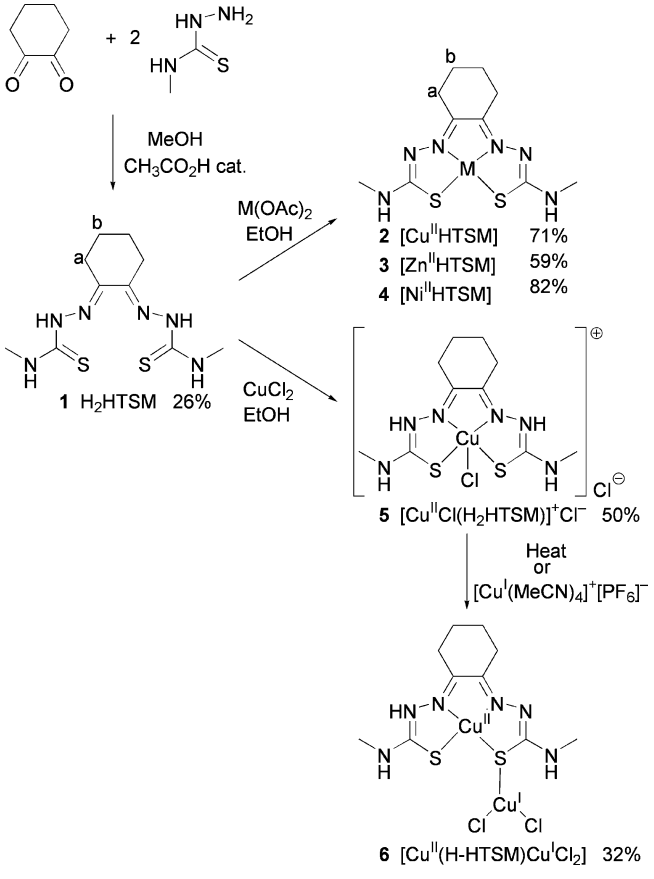

Scheme 1. Synthesis of the H_2HTSM proligand **1** and complexation reactions to form the metal(II) complexes **2**–**6**. The labels, "a" and "b" refer to the methylene (CH_2) groups of the cyclohexane ring as described in the Experimental Section.

Selected experimental and DFT-calculated geometric parameters for compound **1** and copper(II) complex **2** are given in Table 1. The X-ray crystal structure of proligand **1** is shown in Figure 1. In the solid state, the cyclohexane ring lies in an envelope (half-chair) conformation with the four nitrogen atoms N1–N4 and the four carbon atoms C2, C3, C6 and C9 lying coplanar. Carbon atom C7 is displaced above the plane with the dihedral angle *d*(N2–C2–C6–C7) of 157.4°. The carbon–carbon bond length between C2 and C3 is 1.480(2) Å, which is the shortest bond within the cy-

Table 1. Selected experimental (X-ray) and calculated (DFT) geometric parameters for the proligand **1** and copper(II) complex **2**. X-ray crystal structure values with estimated standard deviations (esd values) are presented first followed by the calculated values from DFT geometry optimisations.

Parameter[a]	H_2HTSM proligand, **1**		[Cu^{II}HTSM], **2**	
	Exp. (esd)	Calcd.	Exp. (esd)	Calcd.
r(C1–N1)	1.370(2)	1.376	1.319(5)	1.331
r(N1–N2)	1.3580(19)	1.347	1.378(4)	1.350
r(N2–C2)	1.294(2)	1.302	1.309(5)	1.304
r(C1–N5)[b]	1.325(2)	1.342	1.346(5)	1.352
r(C1–S1)	1.6780(17)	1.686	1.754(4)	1.768
r(Cu–S1)	–	–	2.249(1)[c]	2.290
r(Cu–S2)	–	–	2.249(1)[c]	2.290
r(M–N2)	–	–	1.954(3)[c]	2.005
r(M–N3)	–	–	1.954(3)[c]	2.005
a(C1–N1–N2)	119.06(14)	122.3	110.1(3)	111.8
a(S1–C1–N1)	119.13(13)	118.6	126.7(3)	126.6
a(M–S1–C1)	–	–	94.25(12)	93.8
a(N2–Cu–S1)	–	–	84.73(9)[c]	84.4
a(N2–Cu–N3)	–	–	80.63(17)	80.1
a(N3–Cu–S2)	–	–	84.73(9)[c]	84.4
a(S1–Cu–S2)	–	–	110.42(5)	111.1
RMSD[d]	0.202		0.069	

[a] Bond lengths and distances are given in Å, and bond angles in degrees [°]. [b] Equivalent to *r*(C1–N3)/Å for complex **2**. [c] Related by twofold rotation. [d] Weighted root-mean-square deviation (RMSD) in Å, calculated by using all non-hydrogen atoms between the X-ray crystal structure and the DFT-optimised gas-phase geometry.

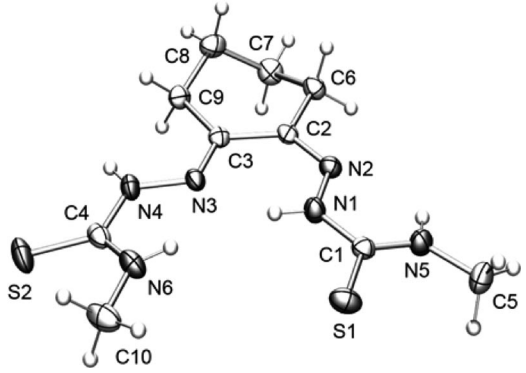

Figure 1. ORTEP[24] representation of the X-ray crystal structure of proligand **1**. Thermal ellipsoids are shown at 50% probability.

clohexane ring and is the same as the average bond length expected for a single bond between two sp^2-hybridised carbon atoms.[23] Each of the six nitrogen atoms have trigonal-planar geometry, indicating sp^2 hybridisation, and all *r*(C–N), *r*(C=S), and *r*(N–N) bonds are intermediate in length between average distances expected for single and double bonds.[23] This structure is consistent with the extensive delocalisation of electron density expected for conjugated bis(thiosemicarbazonato) systems. In contrast with reported crystal structures of other bis(thiosemicarbazone) proligands including H_2ATSM,[20] lack of free rotation about the C2–C3 bond forces the two thiosemicarbazone branches to adopt a *cis* conformation. The *cis* geometry means that the proligand is pre-organised for metal complexation.

The ^{1}H NMR spectrum of proligand **1** (300 MHz in $CDCl_3$ at 295 K) exhibits two unresolved multiplets at δ = 2.50 and 1.75 ppm assigned to the *a*-CH_2 and *b*-CH_2 groups of the cyclohexane ring system, respectively. Two overlapping doublets occur at δ = 3.18 and 3.23 ppm ($^3J_{HH}$ = 4.8 Hz) corresponding to the NHC*H*$_3$ groups which couple to the two broad N*H*CH_3 resonances at δ = 7.30 and 7.51 ppm, respectively. The N^1–*H* and N^4–*H* resonances occur at δ = 12.92 and 8.79 ppm, respectively. The signal of the hydrogen atom bonded to N1 is shifted downfield by intramolecular hydrogen bonding with the lone pair of electrons on N3. The ^{13}C{^{1}H} NMR spectrum shows two resonances assigned to the *a*-*C*H_2 groups at δ = 25.8 and 33.4 ppm, and two resonances due to the *b*-*C*H_2 groups at δ = 21.3 and 22.5 ppm, highlighting the asymmetry within the cyclohexane ring system. The signals of the two NH*C*H_3 terminal methyl groups are observed at δ = 30.9 and 31.9 ppm. Four quaternary carbon resonances are observed and assigned to the two C=N imine groups at δ = 137.2 and 144.3 ppm and two overlapping C=S resonances at δ = 178.2 and 178.4 ppm. The NMR spectra confirm that the most favourable conformation of proligand **1** in chloroform at room temperature has two inequivalent 4-methylthiosemicarbazone groups with four inequivalent N–H groups, and is consistent with the solid-state structure (Figure 1).

DFT calculations are in excellent agreement with the experimental structure of proligand **1**. The weighted root-mean-square deviation (RMSD) calculated for all non-hydrogen atoms, between the X-ray crystal structure and the DFT-optimised gas-phase geometry of proligand **1** is only 0.202 Å (Table 1).

The neutral metal(II) complexes **2**–**4** were isolated from the reaction of proligand **1** with copper, zinc or nickel acetates in hot ethanol. The X-ray crystal structure of red/brown complex **2** is shown in Figure 2. The complex is situated on a crystallographic twofold axis of rotation. With the exception of the sulfur atom, S1, and the methylene carbon atom C6, all non-hydrogen atoms are approximately coplanar. The sulfur atom S1, deviates from the plane-of-best-fit by 0.16 Å, and the carbon atom C6 is displaced by 0.38 Å. The backbone carbon–carbon *r*(C2–C3) decreases slightly on complexation with copper(II) ions to 1.477(7) Å. The weighted RMSD between the experimental and DFT-optimised structure is 0.069 Å, which demonstrates the high level of structural accuracy that can be achieved using modern quantum chemistry programs. Crystal structures of related zinc(II) complexes have been reported previously.[22]

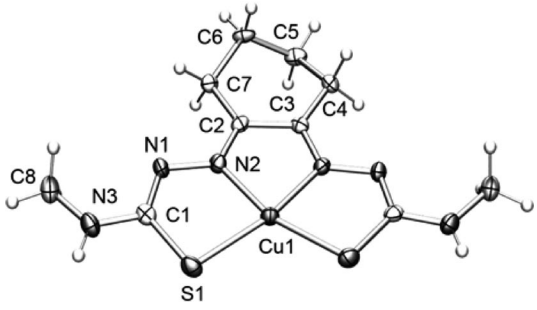

Figure 2. ORTEP[24] representation of the X-ray crystal structure of complex **2**. Thermal ellipsoids are shown at 50% probability, and hydrogen atoms have been omitted for clarity.

In contrast to the complexation reactions with metal(II) acetates, reaction of proligand **1** with copper dichloride dihydrate in ethanol afforded the cationic dark green complex **5** in 50% yield (Scheme 1). This pseudo-square-pyramidal coordination complex remains diprotonated with a bound chlorido ligand in the apical site and a chloride counterion.

Interestingly, when a sample of complex **5** was heated under reflux in acetonitrile and then cooled slowly to room temperature, both a green precipitate and small black crystals (complex **6**) formed. The green powder was found to be complex **5**. However, the X-ray crystal structure of complex **6** is shown in Figure 3, and elemental analysis was consistent with the empirical formula $C_{10}H_{17}Cl_2Cu_2N_6S_2$, corresponding to the neutral complex, [Cu^{II}(H-HTSM)-Cu^{I}Cl$_2$]. Positive ion electrospray mass spectrometry, MS-ES(+ve), gave peaks at *m*/*z* = 348.0247, corresponding to the cationic species {[Cu^{II}HTSM] + H$^+$} (calculated mass 348.0252), and at *m*/*z* = 695 and 1044 indicating the pre-

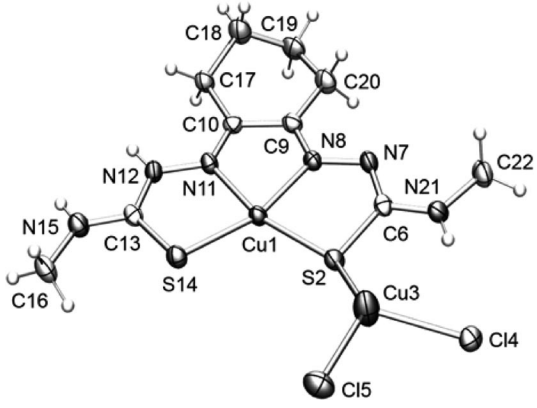

Figure 3. ORTEP[24] representation of the asymmetric unit of the X-ray crystal structure of complex **6**. Thermal ellipsoids are shown at 50% probability, and hydrogen atoms are shown to demonstrate the mono-protonation of the HTSM ligand. Further discussion of the X-ray crystal structure of complex **6** is presented in the Supporting Information.

sence of the protonated dimer {$[Cu^{II}HTSM]_2 + H^+$} and protonated trimer {$[Cu^{II}HTSM]_3 + H^+$}. Complex **6** was also synthesised as a black powder from the reaction of complex **5** with 1 equiv. of [tetrakis(acetonitrile)copper(I) hexafluorophosphate, $[Cu^{I}(CH_3CN)_4]^+[PF_6]^-$, under nitrogen in refluxing, deoxygenated acetonitrile for 1 h.

Copper-64 Radiolabelling

In order to demonstrate the potential use of complex **2** as a radiopharmaceutical, the copper-64 radiolabelled complex, ^{64}Cu-**2** was prepared in aqueous solution by the reaction of proligand **1** with $^{64}Cu(CH_3CO_2)_2$(aq.). A solution of the proligand **1** (50 μL taken from a stock solution of 1 mg in 1 mL of DMSO) was stirred at room temperature with 200 μL of $^{64}Cu(CH_3CO_2)_2$(aq.) in 400 μL of deionised water. After a reaction time of 10 min, a single peak was observed in the reverse phase radio-HPLC (retention time R_t = 14.42 min; $\log P_c = 2.00 \pm 0.35$), and the radiochemical yield of ^{64}Cu-**2** was found to be >98%. Further in vitro and in vivo radiochemical studies are underway to assess the hypoxia selectivity of complex **2**.

Density Functional Theory Calculations

After observing the difference in geometry between the X-ray crystal structure of proligand **1** and other bis(thiosemicarbazones), such as the proligand H_2ATSM, it was of interest to investigate the relative stabilities of different conformations using DFT.[25] The structures of five conformers (**I**–**V**) of the proligand H_2ATSM were optimised using Gaussian03 with the restricted B3LYP exchange-correlation functionals and the double-ζ 6-31++G(d,p) all-electron basis set.[26] Table 2 shows the optimised geometries and relative energies of conformers **I**–**V**. Conformer **V** was identified as the global minimum on the gas-phase potential energy surface and has the same geometry as proligand **1** (Figure 1). The increased stability of conformer **V** is mainly due to intramolecular hydrogen bonding. However, the small energy difference between conformers **I**–**V**, and the increased conformational flexibility due to free rotation about the carbon–carbon backbone means unlike proligand **1**, H_2ATSM is likely to exist as a mixture of conformers at room temperature in solution.

Table 2. DFT-optimised structures and relative gas-phase energies of five conformers **I**–**V** of the proligand, H_2ATSM.

	Calcd. E_{SCF} / kJ mol^{-1}	Optimised geometry
I	73.1	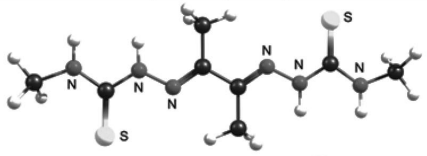
II	127.7	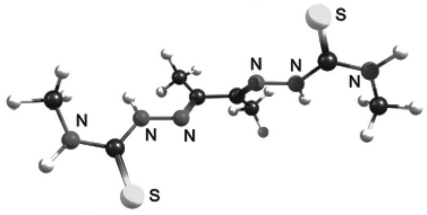
III	74.2	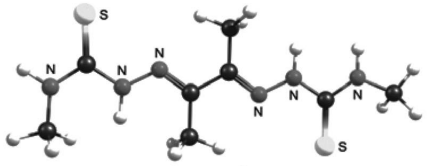
IV	16.6	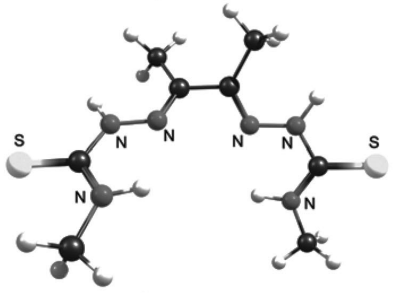
V	0.0	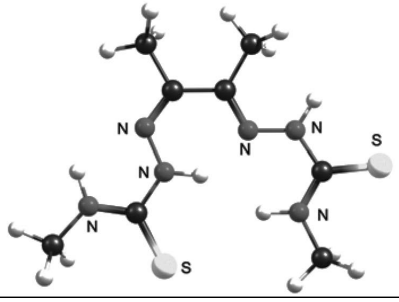

Electrochemistry

Dearling et al. demonstrated that the hypoxia selectivity of bis(thiosemicarbazonato)copper(II) complexes appears to correlate with the one-electron half-wave, $E_{1/2}$/V, reduction potentials.[27,28] Complexes with electron-donating alkyl substituents on the ligand backbone were found to have more negative reduction potentials, and structure–activity relationship studies suggest that complexes with $E_{1/2} \leq -0.58$ V are likely to be hypoxia-selective. Recent DFT calculations of solution-phase reduction potentials and absolute acidities support this conclusion and showed that electron-donating substituents reduce the stability of the copper(I) anion with respect to protonation and ligand dissociation.[28,29]

A key step in the proposed mechanisms of hypoxia selectivity is the reversibility of the one-electron reduction reaction.[15,16,27,28,30] However, the nature of copper(I) complex and its reaction with dioxygen is not well understood. Therefore, the electrochemistry of complex **2** has been studied by using CV and UV/Vis-SEC experiments. All potentials are reported relative to the saturated calomel electrode (SCE) and were corrected using the reversible one-electron oxidation of ferrocene as an internal reference.[31]

The full sweep width CV of a 1.0 mM solution of complex **2** recorded in anhydrous, deoxygenated dimethylformamide (DMF) at room temperature, and the scan-rate dependence

of the reduction couple are presented in Figure 4(a) and (b), respectively. Complex **2** undergoes a quasi-reversible metal-centred one-electron reduction at $E_{1/2}$(SCE) = –0.654 V, with a peak current ratio of $|i_{pa}|/|i_{pc}|$ = 0.995 and a peak separation of ΔE_p = 0.087 V. In the same experimental setup, [Cu^{II}ATSM] was found to have a half-wave potential of –0.646 V, which suggests that on the basis of redox potential, complex **2** is potentially hypoxia-selective. The diffusion coefficients of the oxidised and reduced species involved in the reduction couple were calculated using the Randles-Sevcik equation and were found to be D_O = 6.5×10^{-6} cm^2 s^{-1} and D_R = 7.6×10^{-6} cm^2 s^{-1}, respectively [Equation (1)].

$$i_p = 0.4463nF\,(nF/RT)^{1/2}\,AD^{1/2}Cv^{1/2} \quad (1)$$

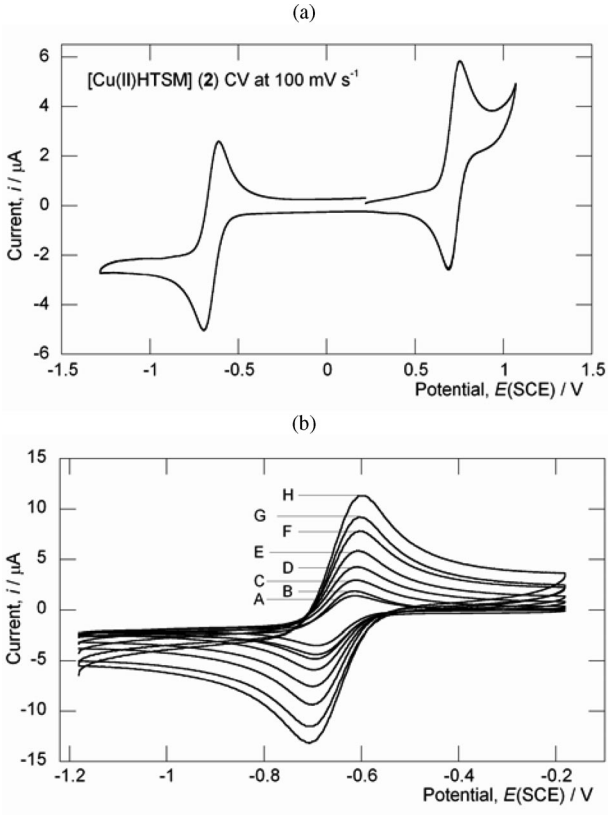

Figure 4. (a) Full sweep width CV of a 1.0 mM solution of complex **2** in anhydrous deoxygenated DMF at room temp. (b) Scan-rate dependence of the metal-centred one-electron reduction couple at (A) 50, (B) 75, (C) 100, (D) 150, (E) 250, (F) 400, (G) 600 and (H) 800 mV s^{-1}.

DFT calculations on the copper(II) complex **2** and the corresponding reduced copper(I) anion, [Cu^{I}HTSM]$^-$ have been conducted to predict the solution-phase reduction potential. Redox potentials were calculated using dimethyl sulfoxide (DMSO, ε = 46.7, R_{solv} = 2.455 Å), water (ε = 78.39, R_{solv} = 1.385 Å) and DMF (ε = 36.7, R_{solv} = 2.67 Å) polarisable continuum solvation models (PCM), where ε is the solvent dielectric constant and R_{solv} is the solvent probe sphere radius. Full details of the calculation methods used have been reported previously.[32] DFT-calculated reduction potentials using the DMSO, water and DMF models were found to be –0.693, –0.531 and –0.594 V, respectively. The calculated values are in reasonably good agreement with the experimental value determined from the CV. However, the calculation of redox potentials appears to be highly sensitive to both the solvent probe size and polarisability.

Figure 5 shows the spatial distributions of the β-spin lowest unoccupied molecular orbital (LUMO) of the optimised neutral copper(II) complex **2** which accepts the electron on reduction and becomes the highest occupied molecular orbital (HOMO) of the reduced copper(I) anion, [Cu^{I}HTSM]$^-$. The coordination geometry of the copper ion changes from square-planar in the neutral copper(II) complex to pseudo-tetrahedral in the copper(I) anion, which is consistent with the quasi-reversible behaviour observed in the CV.

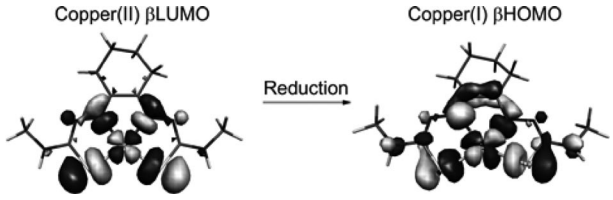

Figure 5. Molecular-orbital isosurfaces showing the spatial distribution of the neutral [Cu^{II}HTSM] (**2**) βLUMO and the anionic [Cu^{I}HTSM]$^-$ βHOMO. On reduction the coordination geometry is predicted to change from square-planar to pseudo-tetrahedral and the dihedral angle *d*(N=C–C=N) opens from 0.0° in the copper(II) species to 23.0° in the copper(I) anion.

Although not thought to be involved in the mechanism of hypoxia selectivity, the quasi-reversible one-electron oxidation potential of complex **2** occurs at $E_{1/2}$(SCE) = +0.721 V, with a peak current ratio of $|i_{pc}|/|i_{pa}|$ = 0.839 and a peak separation of ΔE_p = 0.068 V. The oxidative couple has previously been assigned as a metal-centred Cu^{II}/Cu^{III} process. However, unlike the reduction couple, the oxidation potentials of a range of bis(thiosemicarbazonato)-copper(II) complexes are less sensitive to variations in the relative electron-donating/withdrawing ability of the ligand substituents.[28] DFT calculations indicate that in solution phase using a DMF polarisable continuum solvation model, ligand-based ππ* oxidation of complex **2** to form the oxidised triplet-**2**$^+$ species is thermodynamically more favourable than metal-based oxidation to give the formally copper(III) singlet-**2**$^+$ species by change in electron attachment free energy, $\Delta\Delta G_{EA}$ = –26.1 kJ mol^{-1} at 298 K.[32]

UV/Vis Spectroelectrochemistry

Changes in the electronic absorption spectrum of complex **2** were measured during in situ electrochemical reduction of a 1.0 mM solution in anhydrous, deoxygenated DMF at room temperature, by using an optically transparent thin-layer electrode (OTTLE) cell.

Figure 6(a) shows the changes observed in the electronic absorption spectrum between 800 and 270 nm, during electrochemical reduction of complex **2** at an applied potential of $E_{appl.}$ = –1.181 V. The initial UV/Vis spectrum of complex **2** is very similar to the spectra of related bis(thiosemicarbazonato)copper(II) complexes[33] which were assigned by using time-dependent DFT calculations.[20] During electrochemical reduction, six well-defined isosbestic points are observed at 575, 422, 385, 346, 331 and 291 nm, which demonstrates that reduction proceeds cleanly in deoxygenated DMF to give a single, reduced copper(I) species. The solution changes colour from red to yellow as the peak absorbance at 486 nm (ε = 7545 $M^{-1}cm^{-1}$) decreases during reduction. The absorbance increases in the region between 790 and 575 nm, and two new weaker absorption bands appear at longer wavelengths with peaks at 505 nm (ε = 1340 $M^{-1}cm^{-1}$) and 626 nm (ε = 1220 $M^{-1}cm^{-1}$). At shorter wavelengths, both the intense peak and shoulder in the spectrum of complex **2** at 316 nm (ε = 23600 $M^{-1}cm^{-1}$) and 353 sh nm (ε = 13200 $M^{-1}cm^{-1}$), associated with metal-to-ligand charge transfer and ligand-based ππ* transitions, undergo a redshift and a decrease in absorbance on reduction to give a peak at 331 nm (ε = 17800 $M^{-1}cm^{-1}$) and shoulder at 381 nm (ε = 6700 $M^{-1}cm^{-1}$).

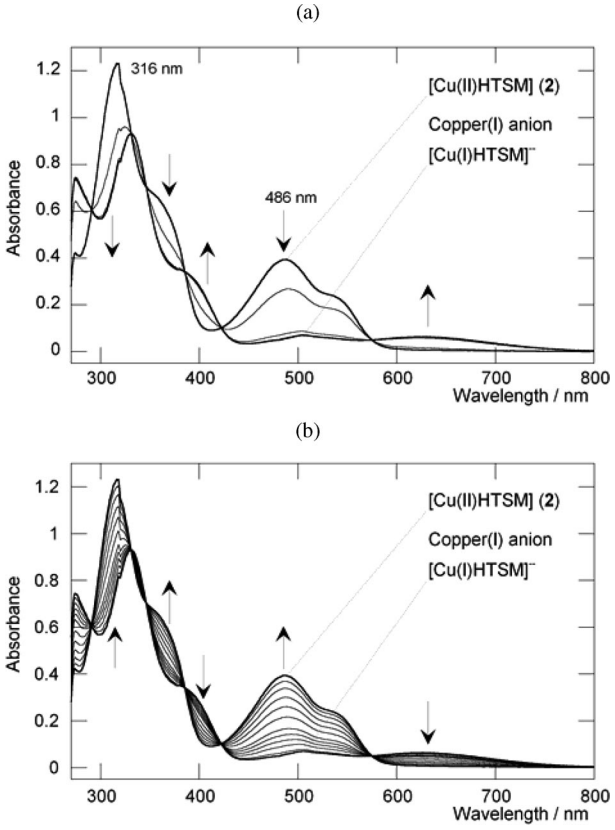

Figure 6. (a) Change in the experimental UV/Vis absorption spectrum of a 1.0 mM solution of complex **2** in anhydrous, deoxygenated DMF during electrochemical reduction at $E_{appl.}$(SCE) = –1.181 V. Bulk electrolysis was performed for 405 s, until the final current was i = 5.0% of the initial current passed at time t = 0 s. The arrows indicate the direction of change in absorbance from the initial spectrum of complex **2** to the spectrum of the reduced copper(I) species. (b) Change in the UV/Vis spectrum observed after electrochemical reduction at open circuit (no potential). After 25 min, the peak absorbance at 486 nm returned to >99% of the initial absorbance of complex **2**.

Although CV and electronic absorption spectroscopy do not provide definitive empirical evidence for the structure of the reduced copper(I) species, the increase in absorbance at wavelengths >575 nm is consistent with the DFT-predicted change from square-planar to pseudo-tetrahedral coordination geometry on reduction (Figure 5).[32] Therefore, the species formed on reduction is the anionic copper(I) complex, $[Cu^{I}HTSM]^{-}$.

Figure 6(b) shows the change in the UV/Vis spectrum of $[Cu^{I}HTSM]^{-}$ after electrochemical reduction. An immediate increase in absorbance at 486 nm was observed, and again, six well-defined isosbestic points developed at the same wavelengths as for the reduction step. After <20 min, the UV/Vis spectrum was indistinguishable from that of the initial spectrum of complex **2**, and the peak absorbance at 486 nm returned to >99% of the initial absorbance. This rapid increase in absorbance is due to the solution-phase oxidation of the copper(I) anion by reaction with dioxygen diffusing into the optical window. Even though the solutions were deoxygenated by a vigorous nitrogen purge and the apparatus was sealed with a Teflon lid and Parafilm, a small amount of dioxygen, which is highly soluble in DMF, is likely to remain present in solution. Background experiments also confirmed that diffusion of complex **2** from the bulk solution into the optical window was slow in comparison to the diffusion and reaction with dioxygen.

In these experiments, the onset of the one-electron reduction of dioxygen to give superoxide radical anions in aerated DMF was found to occur at approximately –0.48 V with a peak at –0.80 V, which is in agreement with previously studies.[34,35]

Despite the central importance of the oxidation of the reduced copper(I) species in the mechanisms of hypoxia selectivity proposed by Fujibayashi et al.[15,16] and Dearling et al.[27,28] the oxidation of $[Cu^{I}HTSM]^{-}$ by dioxygen observed in the UV/Vis-SEC studies provides the first experimental evidence of the feasibility of this reaction. In order to provide further support, DFT calculations were used to predict the energetics of the gas- and solution-phase reaction between $[Cu^{I}HTSM]^{-}$ and dioxygen to give complex **2** and superoxide radical anions [Equation (2)]. Full DFT-calculated energetics are presented in the Supporting Information. The reaction was predicted to be non-spontaneous in the gas phase with a calculated change in the reaction free energy of $\Delta_r G^0$ = +235.5 kJ mol^{-1}, with $\Delta_r H^0$ = 241.9 kJ mol^{-1} and $\Delta_r S^0$ = +21.5 J K^{-1} mol^{-1}. However, when PCM solvation models were included in the self-consistent reaction field (SCRF) calculations, the reaction was found to become thermodynamically feasible with calculated $\Delta_r G^0$(sol) values of –24.0, –8.1 and –25.0 kJ mol^{-1} using water, DMSO and DMF models, respectively.

$$[Cu^{I}HTSM] + O_2 \xrightarrow{\Delta_r G^0(sol)} [Cu^{II}HTSM] + O_2^{-} \quad (2)$$

Electron Paramagnetic Resonance Spectroscopy

The solution-phase EPR spectra of a 1.0 mM solution of complex **2** in anhydrous DMF at room temperature and 100 K are shown in Figure 7(a) and (b), respectively. The room-temperature spectrum was simulated with EasySpin by using the fast-motion regime.[36] From the best fit between the experimental and simulated spectra, the m_I-dependent Lorentzian line-broadening parameters were determined and found to be a = 2.400, b = 1.347 and c = 0.512 with g_{iso} = 2.057, and a copper-63 hyperfine coupling constant, A_{iso}(Cu), of 92.5 G. The observed splitting pattern with 1:2:3:2:1 line intensities occurs due to superhyperfine coupling of the metal-centred unpaired electron with the two equivalent donor nitrogen atoms [A_{iso}(N) = 16 G].

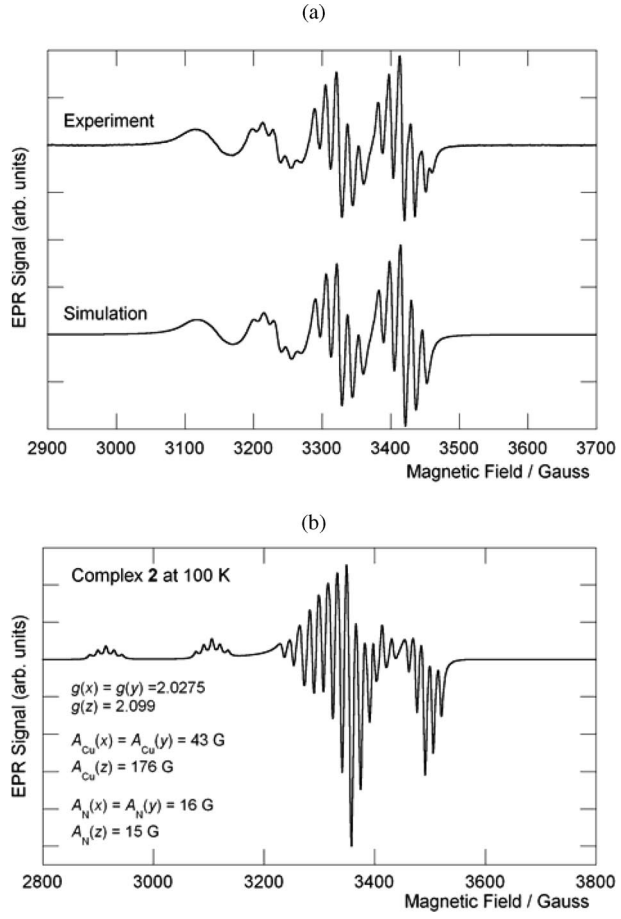

Figure 7. (a) Solution-phase room-temperature experimental and simulated EPR spectrum of a 1.0 mM solution of complex **2** in anhydrous DMF. The simulation was performed by using EasySpin with only copper-63 isotope model.[36] Minor differences between the experimental and simulated spectra are assigned to the presence of copper-65 isotope in natural abundance. (b) Frozen-solution EPR spectrum recorded at 100 K. The spectrum was simulated by using Bruker Win-EPR SimFonia[37] with ^{63}Cu and ^{65}Cu isotopes in natural abundance.

The room-temperature spectrum of complex **2** is consistent with previously reported spectra of related bis(thiosemicarbazonato)copper(II) complexes which indicates that these species adopt the same square-planar coordination geometry in solution.[20,25,33,38] The low value of g_{iso} = 2.057 is also indicative of the covalent nature of bonding in complex **2** and is a consequence of the presence of two soft sulfur donor atoms.

IR and Raman Spectroscopy

Relatively few studies on the IR and Raman spectra of bis(thiosemicarbazonato) complexes have been performed, and calculations have not been used previously to help in the assignment of vibrational spectra.[38–41] Vibrational spectra of systems like complex **2** are difficult to assign due to the extensive π-delocalisation of electron density in the ligand and the large number of combination modes that arise from the coupling of functional group vibrational modes with ring modes from the three five-membered metallocycles formed on metal complexation. Consequently, the fingerprint region between 500 and 1650 cm^{-1} in the IR and Raman spectra are difficult to interpret without calculations.

Figure 8(a) and (b) show the overlay of the experimental powder-phase Raman spectrum and the IR (KBr disc) spec-

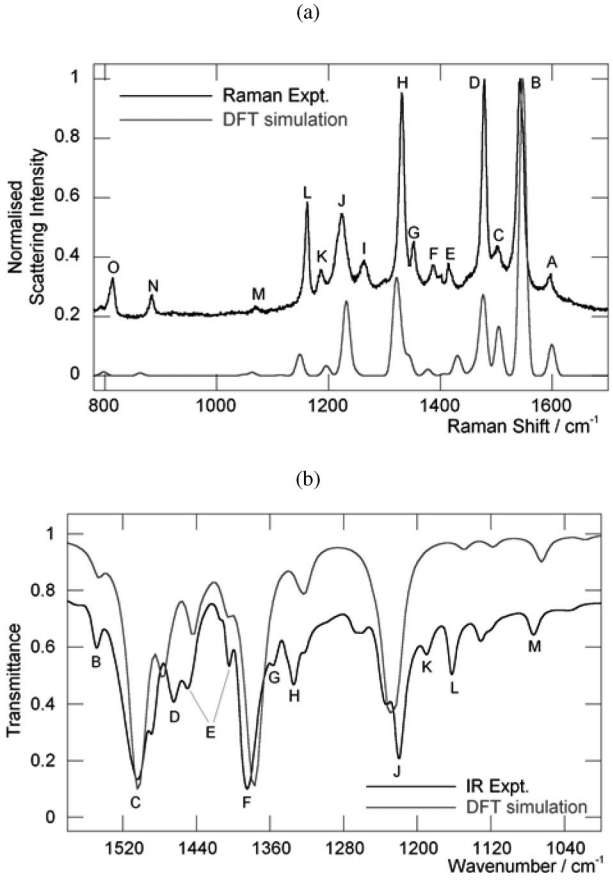

Figure 8. (a) Experimental and DFT-simulated Raman spectra of complex **2** recorded by using an excitation wavelength of 632 nm. The spectra have been normalised to the intensity of the most intense peak and are shifted vertically for clarity. (b) Experimental and DFT-simulated IR spectrum (recorded as a KBr disc) of complex **2**. DFT assignments of vibrational bands A–O are presented in Table 3 and the pictorial representations of the vibrational modes are given in the Supporting Information.

Table 3. Experimental and DFT-calculated Raman and IR absorption bands of complex **2**.

Band	Exp. Raman bands[a] [cm^{-1}]	Calcd. Raman bands[b] [cm^{-1}]	Exp. IR bands[c] [cm^{-1}]	Calcd. IR bands[b] [cm^{-1}]	Assignment[d]
A	1597 w	1598 mw	–	–	υ_{as} (C=N backbone)
B	1543 vs	1547 vs	1549 w	1547 vw	υ_s (C=N backbone) and ring breathing combination
C	1501 mw	1504 mw	1504 vs	1504 vs	δ_{as} and δ_s (N–H)
D	1478 vs	1476 m	1465 m	1478 m	υ_s (NH–C=N) amide stretching mode
E	1414 w	1430 w	1450 m/ 1405 mw	1446 mw/ 1406 w	Raman: δ_{as} (CH_3) and δ_{as} (*a*-CH_2, cyclohexyl)
F	1385 w	1378 vw	1385 vs	1378 vs	υ_s and υ_{as} (NH–C=N) amide stretching mode and δ_{as} (CH_3)
G	1351 mw	1342sh mw	1357 mw	–	δ (mainly *b*-CH_2 cyclohexyl)
H	1330 vs	1321 m	1335 m	1324 mw	υ_s (C–C backbone) with δ (C–H, cyclohexyl)
I	1263 mw	–	–	–	–
J	1224 m	1231 m	1220 s	1229 s	υ_{as} (N–N) with δ (*a*-CH_2, cyclohexyl)
K	1186 w	1195 w	1189 w	–	υ_s (N–N) with δ (ring deformations and CH_3 bending)
L	1161 m	1148 mw	1162 mw	1150 vw	δ (CH_2 cyclohexyl)
M	1070 vw	1063 vw	1074 w	1065 w	δ (ring deformation mode) combined with δ (CH_2 cyclohexyl) and δ (CH_3)
N	884 w	862 vw	884 vw	904 w	δ_s (ring deformation mode) combined with δ (CH_2 cyclohexyl)
O	814 w	798 vw	814 vw	791 w	υ_s (Cu–N) with υ_s (C–S) and δ (cyclohexyl ring breathing)

[a] Calculated vibrational frequencies have been scaled by a factor of 0.97.[43] [b] Relative peak intensities are indicated by the symbols: vs = very strong, s = strong, m = medium, w = weak, vw = very weak, sh = shoulder. [c] Stretching and deformation modes are denoted by the symbols: υ and δ (subscripts "s" and "as" refer to symmetric and antisymmetric normal vibrational modes, respectively). [d] The intense peak observed at 1330 cm^{-1} in the Raman spectrum (Band H) is assigned mainly to the C–C backbone stretching mode.

trum of complex **2** with the DFT-calculated vibrational spectra. The Raman spectrum was recorded by using an excitation wavelength of 632 nm. The DFT-calculated IR and Raman spectra were simulated with the SWizard program[42] by using a Lorentzian band shape and a global half-band width of 15 cm^{-1}. Energies of the B3LYP/6-31++G(d,p) calculated vibrational bands have been scaled by using an optimal vibrational scaling factor of 0.97.[43] Details of the assignment of vibrational bands A–O (Figure 8) are presented in Table 3 and the Supporting Information.

The region between 60 and 800 cm^{-1} in the Raman spectrum of complex **2** exhibits more than 20 sharp, low-intensity peaks. DFT calculations indicate that the majority of these vibrations involve large contributions from both ring breathing and rocking modes of the three metallocycles, and C–H deformations of the methyl and cyclohexyl groups.[41] The experimental Raman spectrum shows two low-intensity peaks at 814 and 765 cm^{-1}, which are assigned to the symmetric and asymmetric Cu–N_{donor} stretching modes (calculated frequencies of 790 and 769 cm^{-1}, respectively) in combination with both symmetric C–S stretching and cyclohexyl ring breathing modes. As expected, the Cu–S stretching modes occur at lower frequencies but are more difficult to assign due to strong combinations with both CH_2 deformations and metallocycle ring breathing modes. Therefore, the symmetric Cu–S stretching mode is tentatively assigned to either of the sharp, medium-intensity peaks in the expermental spectrum at 433 or 328 cm^{-1}, with the calculated vibrational mode lying between these two peaks at 388 cm^{-1}. The asymmetric Cu–S stretching mode gives a dominant contribution to the calculated vibrational modes at 286 and 261 cm^{-1}, and is assigned to two peaks of equal intensity at 304 and 269 cm^{-1} in the experimental Raman spectrum.

This DFT assignment of the vibrational modes in the spectra of complex **2** is in good agreement with the assignment of the Raman spectrum of the related bis(thiosemicarbazonato)copper(II) complex, [Cu^{II}KTS], reported by Tosi et al.[41] They also reported that when excited in the visible region of the spectrum around 450 nm, bis(thiosemicarbazonato)copper(II) complexes fluoresce with a peak emission around 550 nm. This copper(II) fluorescence emission is much weaker than the fluorescence observed for the analogous bis(thiosemicarbazonato)zinc(II) complexes and is not observed by using conventional fluorescence spectrophotometers or microscopes.[20,44] Fluorescence emission was also detected in the Raman spectrum of complex **2**, which showed a distinct curvature in the baseline (Supporting Information). Further investigations aimed at improving the fluorescence quantum yield and probing the mechanisms of cellular uptake, localisation and hypoxia selectivity of bis(thiosemicarbazonato)copper(II) complexes are underway in Oxford.

Summary and Conclusions

Metal(II) complexes of the 1,2-cyclohexanedione bis(4-methylthiosemicarbazone) ligand have been synthesised and investigated as potential hypoxia-selective copper radiopharmaceuticals. A range of spectroscopic techniques have been used to characterise the potential copper radiopharmaceutical, including UV/Vis, IR, Raman and EPR spectroscopy. The vibrational spectra have been assigned by using DFT calculations. Spectroelectrochemistry experi-

ments have shown that metal-centred one-electron reduction gives the anionic copper(I) species, $[Cu^{I}HTSM]^{-}$, which is stable in the absence of a proton source. The oxidation of the copper(I) anion by dioxygen has been observed, which provides new evidence in support of the proposed mechanisms of hypoxia selectivity.[15,27,28,45] Density functional theory calculations have also been used to study the potential energy surface of bis(thiosemicarbazone) proligands and the electronic structures of the copper(II) and copper(I) species. These results also demonstrate that despite large variations in the ligand backbone structure, the electronic and spectroscopic properties of complex **2** remain very similar to those of the hypoxia-selective radiopharmaceutical, $[Cu^{II}ATSM]$.

The copper(II) complex, $[Cu^{II}HTSM]$, has a one-electron reduction potential which lies within the range expected to confer hypoxia-selective tumour uptake, and the high radiochemical yield of the copper-64 radiolabelled complex means that complex **2** has high potential to be used as a PET imaging agent. Further in vitro cellular studies and in vivo biodistribution studies are underway.

Experimental Section

General: All reagents and solvents were obtained from commercial sources (SigmaAldrich and Lancaster) and, unless otherwise stated, were used as received. Elemental analyses were performed by the microanalysis service of the department at the University of Oxford. NMR spectra were recorded with a Varian Mercury VX300 spectrometer, [^{1}H at 300 MHz, $^{13}C\{^{1}H\}$ at 75.5 MHz] by using the residual solvent signal as an internal reference. Mass spectra were recorded with a Micromass LCT Time of Flight Mass Spectrometer by using positive ion electrospray (ES^{+}). Where possible, accurate masses are reported to four decimal places by using tetraoctylammonium bromide (466.5352 Da) as an internal reference. UV/Vis spectra were recorded with a Perkin–Elmer Lambda 19 UV/Vis/NIR spectrometer. EPR spectra were recorded by using quartz cylindrical cells with a Bruker EMX-micro X-band spectrometer at the EPSRC National EPR Service, at the University of Manchester. High performance liquid chromatography (HPLC) was conducted by using a Gilson HPLC machine equipped with a Hamilton PRP-1 reverse-phase column and UV/Vis detection at 254 nm. Retention times, R_t/min, by using a water/acetonitrile gradient elution method (1.0 mL/min), shown in the Supporting Information, are presented for all compounds. CVs of approximately 1.0 mM solutions of zinc(II) and copper(II) complexes in 5.0 mL of anhydrous dimethylformamide (DMF) were recorded with a CH Instruments Electrochemical Analyser by using a platinum working electrode, a platinum wire counter/auxiliary electrode and a silver/silver ion reference electrode. Ferrocene was used as an internal reference for which the one-electron redox process occurs at $E_{1/2}$ = 0.53 V (DMF) vs. SCE.

Synthesis

1,2-Cyclohexanedione Bis(4-methylthiosemicarbazone) Proligand (H_2HTSM, 1): This compound was synthesised by using a procedure described by Mohan et al.[21] 4-Methylthiosemicarbazide (4.69 g, 44.6 mmol) was added to methanol (60 mL) containing glacial acetic acid (4 mL) and heated for 5 min. This solution was then added to a hot solution of 1,2-cyclohexanedione (2.50 g, 22.3 mmol) in methanol (50 mL). The mixture was heated under reflux for 15 min until a clear yellow solution was produced and was then cooled to room temperature. A yellow crystalline solid formed which was collected by filtration, washed with a 1:1 mixture of methanol/water and dried in vacuo. The product was recrystallised from methanol/water (1:1) and dried in vacuo to give compound **1** as yellow crystals (1.69 g, 5.9 mmol, 26%). $C_{10}H_{18}N_6S_2$ (286.42): calcd. C 41.9, H 6.3, N 29.3; found C 42.0, H 6.4, N 29.4. Solution-phase ^{1}H and $^{13}C\{^{1}H\}$ NMR spectra of proligand **1** were assigned by using two-dimensional COSY, HMQC and HMBC NMR experiments recorded in $CDCl_3$. ^{1}H NMR (300 MHz, $CDCl_3$): δ = 12.92 [s, 1 H, NHC(=S)N(1)*H*N=], 8.79 [s, 1 H, NHC(=S)N(4)*H*N=], 7.51 and 7.20 (2 br. s, 2 × 1 H, N*H*CH_3), 3.23 and 3.18 (2 overlapping d, $^{3}J_{HH}$ = 4.8 Hz, 6 H, NHCH_3), 2.50 (br. m, 4 H, *a*-CH_2), 1.75 (br. m, 4 H, *b*-CH_2) ppm. $^{13}C\{^{1}H\}$ NMR (75.5 MHz, $CDCl_3$): δ = 178.4 and 178.2 (*C*=S), 144.3 and 137.2 (*C*=N), 33.4 (*a*-*C*H_2), 31.9 and 30.9 (NH*C*H_3), 25.8 (*a*-*C*H_2), 22.5 and 21.3 (*b*-*C*H_2) ppm. MS (ES^{+}): *m*/*z* = 287.1102 (calcd. 287.1113) [M + H^{+}]. Crystals suitable for single-crystal X-ray diffraction were isolated from the recrystallised product.

[1,2-Cyclohexanedione bis(4-methylthiosemicarbazonato)]copper(II) ([Cu^{II}HTSM], 2): Synthesised by using a procedure based on that described by Rodriguez-Argüelles et al.[22] Proligand **1** (0.30 g, 1.05 mmol) in ethanol (30 mL) was added to a hot solution of copper(II) acetate monohydrate (0.21 g, 1.05 mmol, 1.0 equiv.) in ethanol (20 mL), and the solution was heated under nitrogen under reflux for 2 h. The reaction mixture was then concentrated under reduced pressure and cooled to room temperature. The precipitate was collected by filtration, washed with hexane (2 × 5 mL) and diethyl ether (2 × 10 mL) and then dried in vacuo to give complex **2** as a red/brown microcrystalline solid (0.26 g, 7.5×10^{-4} mol, 71%). $C_{10}H_{16}CuN_6S_2$ (347.95): calcd. C 34.5, H 4.6, N 24.1; found C 34.5, H 4.6, N 24.1. MS (ES^{+}): *m*/*z* = 348.0247 (calcd. 348.0252) [M + H^{+}]. UV/Vis (DMF): λ_{max}/nm (ε/mol^{-1} dm^{3} m^{-1}) = 532 sh (4742 ± 83), 486 (7545 ± 133), 353 sh (13200 ± 241), 316 (23600 ± 465). HPLC: R_t = 14.42 min. Calcd. log P_c = 2.00 ± 0.35. Crystals suitable for single-crystal X-ray diffraction were grown by slow concentration of a methanol solution.

[1,2-Cyclohexanedione bis(4-methylthiosemicarbazonato)]zinc(II), ([Zn^{II}HTSM], 3): Synthesised by using the same procedure as described for complex **2**.[22] Zinc diacetate dihydrate (0.23 g, 1.05 mmol) was added to a solution of proligand **1** (0.30 g, 1.05 mmol) in ethanol (30 mL). Complex **3** was isolated as a orange/yellow microcrystalline solid (0.22 g, 6.3×10^{-4} mol, 59%). $C_{10}H_{16}N_6NiS_2$ (343.09): calcd. C 35.0, H 4.7, N 24.5; found C 34.9, H 4.7, N 24.4. ^{1}H NMR (300 MHz, [D_6]DMSO): δ = 7.24 (br. s, 2 H, 2 × CH_3N*H*), 2.82 and 2.80 (2 overlapping br. s, 6 H, 2 × *C*H_3NH), 2.61 (m, 4 H, *a*-CH_2), 1.66 (m, 4 H, *b*-CH_2) ppm. $^{13}C\{^{1}H\}$ NMR (75.5 MHz, [D_6]DMSO): δ = 176.2 (br., 2 × *C*=S), 145.0 (br., 2 × *C*=N), 29.3 (2 × *C*H_3), 26.4 (2 × *a*-*C*H_2), 21.3 (2 × *a*-*C*H_2) ppm. MS (ES^{+}): *m*/*z* = 349.0262 (calcd. 349.0248) [M + H^{+}] (100%). HPLC: R_t = 12.15 min.

[1,2-Cyclohexanedione bis(4-methylthiosemicarbazonato)]nickel(II), ([Ni^{II}HTSM], 4): Synthesised by using the same procedure as described for complex **2**.[22] Nickel diacetate tetrahydrate (0.26 g, 1.05 mmol) was added to a solution of proligand **1** (0.30 g, 1.05 mmol) in ethanol (30 mL). Complex **4** was isolated as a purple microcrystalline solid (0.30 g, 8.6×10^{-4} mol, 82%). $C_{10}H_{16}N_6NiS_2$ (343.09): calcd. C 35.0, H 4.7, N 24.5; found C 34.9, H 4.7, N 24.4. ^{1}H NMR (300 MHz, [D_6]DMSO, 40 °C): δ = 9.08 (br. s, 1 H, CH_3N*H*), 7.50 (br. s, 1 H, CH_3N*H*), 3.00 (br. m, 2 H, *b*-CH_2), 2.80 and 2.75 (2 overlapping br. s, 6 H, 2 × *C*H_3NH), 2.38 (br. m, 2 H, *b*-CH_2), 1.61 (br. m, 2 H, *a*-CH_2), 1.54 (br. m, 2 H, *a*-CH_2) ppm.

MS (ES^+): *m*/*z* 343.0299 (calcd. 343.0310) [M + H^+] (100%). HPLC: R_t = 12.81 min.

Chlorido[1,2-cyclohexanedione bis(4-methylthiosemicarbazonato)]-copper(II) Chloride {[$Cu^{II}Cl(H_2$-HTSM)]Cl, 5}: Complex **5** was synthesised by using the same procedure as described for complex **2** but with copper(II) chloride dihydrate (0.18 g, 1.05 mmol) and proligand **1** (0.30 g, 1.05 mmol) in ethanol (30 mL). Complex **5** was isolated as a dark green microcrystalline solid (0.22 g, 5.3×10^{-4} mol, 50%). $C_{10}H_{18}Cl_2CuN_6S_2$ (420.87): calcd. C 28.5, H 4.3, N 20.0; found C 28.2, H 4.1, N 19.7. MS (ES^+): *m*/*z* = 348.0255 (calcd. 348.0252) [M – 2 HCl + H^+].

[1,2-Cyclohexanedione 1-(4-methylthiosemicarbazone) 2-(4-methylsemicarbazonato)]copper(II)–Copper(I) Dichloride {[$Cu^{II}(H_2$-HTSM)Cu^ICl_2], 6}: Complex **6** was prepared by adding complex **5** (0.07 g, 1.7×10^{-4} mol) to a solution of $[Cu^I(CH_3CN)_4]^+[PF_6]^-$ in deoxygenated acetonitrile (20 mL). The reaction mixture was heated under nitrogen under reflux for 1 h, then cooled slowly to room temperature. The precipitate was isolated by filtration and dried in vacuo to give complex **6** as a black microcrystalline solid (0.026 g, 5.3×10^{-5} mol, 32%). $C_{10}H_{17}Cl_2Cu_2N_6S_2$ (483.41): calcd. C 24.9, H 3.5, N 17.4; found C 25.0, H 3.8, N 17.6. Crystals suitable for single-crystal X-ray diffraction were obtained from a solution of complex **5** in deoxygenated acetonitrile. Black crystals were isolated after heating to boiling point and then leaving the solution to cool and concentrate slowly at room temperature.

Vibrational Spectroscopy: IR spectra were recorded as KBr discs by using a Bruker Tensor27 IR spectrometer. Raman spectra of powder samples were recorded with a Jobin Yvon spectrometer (Labram 1B) equipped with a microscope with a 10× magnification objective (Olympus company) by using a 20-mW HeNe laser. Four spectra were collected for 20 s each and the data was averaged to give the final spectrum. Resolution was approximately 1.0 cm^{-1} for scattering below 200 cm^{-1} increasing to around 0.5 cm^{-1} for energies up to 3600 cm^{-1}. The abscissa was calibrated with the 520.7 cm^{-1} peak of a silicon standard, and the sharp Raman shifts are accurate within the limits of the resolution.

UV/Vis Spectroelectrochemistry: UV/Vis-SEC experiments were performed in anhydrous DMF with 0.1 mol dm^{-3} TBA-BF_4 supporting electrolyte, by using a custom-made optically transparent thin-layer electrode (OTTLE) quartz cell (path length: *l* = 0.46 mm), sealed with a Teflon™ cap and Parafilm. The total volume of the OTTLE cell was approximately 4 mL and, unless otherwise stated, 1.0×10^{-3} mol dm^{-3} copper(II) solutions were used. The same auxiliary and reference electrodes as used in the CV measurements were situated in the bulk solution above the optical cavity. A transparent platinum wire mesh (approximately 50 wires per inch, 0.10 mm thickness) was placed inside the optical cavity and was used as the working electrode.

Copper-64 Radiolabelling: Radiolabelling experiments were conducted at the Wolfson Brain Imaging Centre, Addenbrooke's Hospital, Cambridge, UK. Copper-64 was provided as $^{64}CuCl_2$(aq.) in 0.1 mol dm^{-3} HCl. An aqueous solution of copper-64 acetate, $^{64}Cu(CH_3CO_2)_2$, was prepared by diluting 0.2 mL of the $^{64}CuCl_2$(aq.) in 0.1 M HCl with 0.1 M sodium acetate (1.8 mL, pH = 5.5). This stock solution was used for the radiolabelling experiments, and the activity was measured as 78.4 MBq in 2 mL. A standard solution of the proligand **1** was prepared by dissolving 1.0 mg in 1.0 mL of DMSO. Copper-64 radiolabelled complex ^{64}Cu-**2** was prepared by treating $^{64}Cu(CH_3CO_2)_2$ (200 μL, <10 MBq), with 100 μL of the standard solution of proligand **1** and water (400 μL) in a 2 mL reaction vial. The reaction mixtures were stirred at room temperature for 10 min, then 25 μL of the reaction solution was taken for analysis by reverse-phase radio-HPLC. The syringe was washed thoroughly with DMSO and water both before and after use to prevent contamination. All washings were stored behind the lead shield. HPLC analysis was performed by using a Gilson HPLC machine equipped with a 250 mm × 4.6 mm Phenomenox Primesphere 5 C18-HC 110H column. Both UV detection ($\lambda_{obsd.}$ = 254 nm) and NaI scintillation crystal detection were used in series with a delay time of approximately 10 s. A 25 min water/acetonitrile gradient elution method was used (Supporting Information).

Density Functional Theory Calculations: All calculations were conducted by using density functional theory[46,47] (DFT) as implemented in the Gaussian03, Revision C.02 and D.01 suite of ab initio quantum chemistry programs.[26] Geometry optimisations and vibrational frequency calculations were performed with an unrestricted scheme by using the hybrid-DFT uB3LYP exchange-correlation functionals[48–53] and the all-electron double-ζ 6-31++G(d,p) basis set by Pople et al.[54–60] for all atoms. Normal SCF and geometry convergence criteria were used throughout, and no symmetry constraints were imposed. For all of the gas-phase calculations, harmonic-frequency analysis based on analytical second derivatives was used to characterise the optimised geometries as local minima. Simulated IR and Raman spectra were calculated from the DFT frequency output by using the SWizard program[42] with a global half-band width of 15 cm^{-1}. Calculated vibrational energies were scaled by a factor of 0.97.[43] The effects of solvation were incorporated[61,62] iteratively by performing self-consistent reaction field (SCRF) calculations and using the integral equation formalism polarisable continuum model (IEFPCM) initially developed by Tomasi and co-workers.[63] The solute/solvent boundary was defined by using a solvent-excluding surface[64] (SES), and the solute surface was defined by using the United Atom (Hartree–Fock) Topological model (UAHF) for the radii of the solute atoms.[65] Three solvent models were employed: water (ε = 78.39, R_{solv} = 1.385 Å), DMSO (ε = 46.7, R_{solv} = 2.455 Å) and DMF (ε = 36.7, R_{solv} = 2.67 Å),[66] where ε is the dielectric constant and R_{solv} is the sphere radius of the solvent.

X-ray Crystallography: Crystallographic data for all structures determined are given in Table 4. Crystals were mounted on a glass fibre and cooled rapidly to 150 K in a stream of cold N_2 by using an Oxford Cryosystems CRYOSTREAM unit. Diffraction data were measured by using an Enraf–Nonius Kappa CCD diffractometer (graphite-monochromated Mo-K_α radiation, λ = 0.71073 Å). Cell parameters and intensities were corrected for absorption effects by using the multiscan method based on multiple scans of identical reflections, and intensity data were processed by using the DENZO-SMN package.[67] Space groups were identified by examination of the systematic absences in the intensity data. The structures were solved by using the direct methods program SIR92,[68] which located all non-hydrogen atoms. Subsequent full-matrix least-squares refinement was carried out by using the CRYSTALS program suite.[69] Coordinates and anisotropic thermal parameters of all non-hydrogen atoms were refined. The NH hydrogen atoms were located in the difference Fourier map, and their coordinates and isotropic thermal parameters were subsequently refined. Other hydrogen atoms were positioned geometrically after each cycle of refinement. A three-term Chebychev polynomial weighting scheme was applied. Images were generated by using ORTEP-3.[24] CCDC-685641 (for **1**), -685642 (for **2**), -685643 (for **6**) contain the supplementary crystallographic data for this paper. This data can be obtained free of charge from The Cambridge Crystallographic Data Centre via www.ccdc.cam.ac.uk/data_request/cif.

Table 4. Crystallographic data for the proligand **1** and copper(II) complexes **2** and **6**.

	H_2HTSM proligand (**1**)	[Cu^{II}HTSM] (**2**)	[Cu^{II}(H-HTSM)$Cu^{I}Cl_2$] (**6**)
Empirical formula	$C_{10}H_{18}N_6S_2$	$C_{10}H_{16}CuN_6S_2$	$C_{10}H_{17}Cl_2Cu_2N_6S_2$
Formula mass	286.42	347.94	483.41
T [*K*]	150	150	150
λ [Å]	0.71073	0.71073	0.71073
Crystal system	monoclinic	orthorhombic	monoclinic
Space group	$P2_1/n$	*Pbcn*	$P2_1/n$
a [Å]	10.1191(2)	14.9569(6)	13.3921(4)
b [Å]	8.7194(2)	10.1921(4)	7.6541(3)
c [Å]	15.9209(4)	8.8832(3)	16.1897(6)
α [°]	90	90	90
β [°]	100.0975(12)	90	94.1314(17)
γ [°]	90	90	90
V [Å^3]	1383.0	1354.17	1655.20(10)
Z	4	4	4
$D_{calcd.}$ [g cm^{-3}]	1.376	1.707	1.940
Absorption coefficient, μ [mm^{-1}]	0.378	1.916	3.147
F(000)	608.890	717.912	972.00
Size [mm]	$0.18 \times 0.26 \times 0.26$	$0.06 \times 0.08 \times 0.40$	$0.08 \times 0.14 \times 0.30$
Crystal description	pale-yellow block	dark-brown needle	black prism
θ range collected [°]	$5.0 \leq \theta \leq 27.5$	$5.0 \leq \theta \leq 27.5$	$5.0 \leq \theta \leq 27.5$
hkl ranges	$-13 \leq h \leq 12$, $0 \leq k \leq 11$, $0 \leq l \leq 20$	$0 \leq h \leq 19$, $0 \leq k \leq 13$, $0 \leq l \leq 11$	$-17 \leq h \leq 17$, $0 \leq k \leq 9$, $0 \leq l \leq 21$
Reflections measured	13913	10419	16834
Unique reflections	3129	1542	4032
R_{int}	0.033	0.052	0.063
Reflections observed [$I > 2\sigma(I)$]	2262	870	2780
Transmission coefficients (min/max)	0.91/0.93	0.86/0.89	0.64/0.78
Parameters refined	163	87	199
R or *R*1 (observed reflections)	$R = 0.0360$	$R = 0.0355$	$R = 0.0444$
wR or *R*2 (all data)	$wR = 0.0416$	$wR = 0.0362$	$wR = 0.1195$
Goodness of fit (GOF)	1.055	1.100	1.062
Residual electron density (min/max) [e Å^3]	–0.27/0.27	–0.38/0.34	–1.24/0.92

Supporting Information (see footnote on the first page of this article): DFT-calculated vibrational modes; DFT-optimised Cartesian coordinates; reverse-phase HPLC, vibrational spectroscopy; UV/Vis spectroelectrochemistry, X-ray crystal structure of complex **6**.

Acknowledgments

Thanks are due to all members of the J. R. Dilworth and J. C. Green groups at the University of Oxford. J. P. H. thanks the Merton College and the Engineering and Physical Sciences Research Council (EPSRC) for a studentship. P. J. B. thanks GlaxoSmithKline for funding. C. G. S. thanks the Austrian Academy of Sciences for funding. We thank Dr. Paul S. Donnelly for provisional investigations on the radiolabelling of complex **2** and Dr. Franklin I. Aigbirhio for the provision of copper-64 and radiochemistry facilities. We are indebted to Prof. David J. Watkin, Dr. Nick Rees, Mr. Colin Sparrow and Mrs. Maria Marshall for technical support. We also thank the Oxford Supercomputing Centre.

[1] *A framework for the development of positron emission tomography (PET) services in England*, UK Government, **2005**, http://www.dh.gov.uk.
[2] S. V. Smith, *J. Inorg. Biochem.* **2004**, *98*, 1874.
[3] P. Blower, *Dalton Trans.* **2006**, 1705.
[4] C. J. Anderson, M. J. Welch, *Chem. Rev.* **1999**, *99*, 2219.
[5] M. J. Adam, D. S. Wilbur, *Chem. Soc. Rev.* **2005**, *34*, 153.
[6] S. S. Jurisson, J. D. Lydon, *Chem. Rev.* **1999**, *99*, 2205.
[7] M. J. Adam, *J. Labelled Compd. Radiopharm.* **2002**, *45*, 167.
[8] O. Couturier, A. Luxen, J.-F. Chatal, J.-P. Vuillez, P. Rigo, R. Hustinx, *Eur. J. Nucl. Med. Mol. Imaging.* **2004**, *31*, 1182.
[9] H. Yorimitsu, Y. Murakami, H. Takamatsu, S. Nishimura, E. Nakamura, *Angew. Chem. Int. Ed.* **2005**, *44*, 2708.
[10] C. Halldin, B. Gulyas, L. Farde, *Curr. Pharm. Des.* **2001**, *7*, 1907.
[11] J. M. Brown, *Cancer Res.* **1999**, *59*, 5863.
[12] M. F. Adam, E. C. Gabalski, D. A. Bloch, J. W. Oehlert, J. M. Brown, A. A. Elsaid, H. A. Pinto, D. J. Terris, *Head Neck* **1999**, *21*, 146.
[13] D. M. Brizel, G. S. Sibley, L. R. Prosnitz, R. L. Scher, M. W. Dewhirst, *Int. J. Radiat. Oncol. Biol. Phys.* **1997**, *38*, 285.
[14] P. J. Blower, J. S. Lewis, J. Zweit, *Nucl. Med. Biol.* **1996**, *23*, 957.
[15] Y. Fujibayashi, H. Taniuchi, Y. Yonekura, H. Ohtani, J. Konishi, A. Yokoyama, *J. Nucl. Med.* **1997**, *38*, 1155.
[16] A. Obata, S. Kasamatsu, J. S. Lewis, T. Furukawa, S. Takamatsu, J. Toyohara, T. Asai, M. J. Welch, S. G. Adams, H. Saji, Y. Yonekura, Y. Fujibayashi, *Nucl. Med. Biol.* **2005**, *32*, 21.
[17] F. Dehdashti, P. W. Grigsby, M. A. Mintun, J. S. Lewis, B. A. Siegel, M. J. Welch, *Int. J. Radiat. Oncol. Biol. Phys.* **2003**, *55*, 1233.
[18] F. Dehdashti, M. A. Mintun, J. S. Lewis, J. Bradley, R. Govindan, R. Laforest, M. J. Welch, B. A. Siegel, *Eur. J. Nucl. Med. Mol. Imaging.* **2003**, *30*, 844.
[19] J. L. Tatum, G. J. Kelloff, R. J. Gillies, J. M. Arbeit, J. M. Brown, K. S. C. Chao, J. D. Chapman, W. C. Eckelman, A. W. Fyles, A. J. Giaccia, R. P. Hill, C. J. Koch, M. C. Krishna, K. A. Krohn, J. S. Lewis, R. P. Mason, G. Melillo, A. R. Padhani, G. Powis, J. G. Rajendran, R. Reba, S. P. Robinson, G. L. Semenza, H. M. Swartz, P. Vaupel, D. Yang, B. Croft, J. Hoff-

man, G. Liu, H. Stone, D. Sullivan, *Int. J. Radiat. Biol.* **2006**, *82*, 699.
[20] J. P. Holland, F. I. Aigbirhio, H. M. Betts, P. D. Bonnitcha, P. Burke, M. Christlieb, G. C. Churchill, A. R. Cowley, J. R. Dilworth, P. S. Donnelly, J. C. Green, J. M. Peach, S. R. Vasudevan, J. E. Warren, *Inorg. Chem.* **2007**, *46*, 465.
[21] M. Mohan, P. Sharma, M. Kumar, N. K. Jha, *Inorg. Chim. Acta* **1986**, *125*, 9.
[22] M. C. Rodriguez-Arguelles, L. P. Battaglia, M. B. Ferrari, G. G. Fava, C. Pelizzi, G. Pelosi, *J. Chem. Soc., Dalton Trans.* **1995**, 2297.
[23] F. H. Allen, O. Kennard, D. G. Watson, L. Brammer, A. G. Orpen, R. Taylor, *J. Chem. Soc. Perkin Trans. 2* **1987**, S1.
[24] L. J. Farrugia, *J. Appl. Crystallogr.* **1997**, *30*, 565.
[25] P. J. Blower, T. C. Castle, A. R. Cowley, J. R. Dilworth, P. S. Donnelly, E. Labisbal, F. E. Sowrey, S. J. Teat, M. J. Went, *Dalton Trans.* **2003**, 4416.
[26] M. J. Frisch, G. W. Trucks, H. B. Schlegel, G. E. Scuseria, M. A. Robb, J. R. Cheeseman, J. A. Montgomery, Jr., T. Vreven, K. N. Kudin, J. C. Burant, J. M. Millam, S. S. Iyengar, J. Tomasi, V. Barone, B. Mennucci, M. Cossi, G. Scalmani, N. Rega, G. A. Petersson, H. Nakatsuji, M. Hada, M. Ehara, K. Toyota, R. Fukuda, J. Hasegawa, M. Ishida, T. Nakajima, Y. Honda, O. Kitao, H. Nakai, M. Klene, X. Li, J. E. Knox, H. P. Hratchian, J. B. Cross, V. Bakken, C. Adamo, J. Jaramillo, R. Gomperts, R. E. Stratmann, O. Yazyev, A. J. Austin, R. Cammi, C. Pomelli, J. W. Ochterski, P. Y. Ayala, K. Morokuma, G. A. Voth, P. Salvador, J. J. Dannenberg, V. G. Zakrzewski, S. Dapprich, A. D. Daniels, M. C. Strain, O. Farkas, D. K. Malick, A. D. Rabuck, K. Raghavachari, J. B. Foresman, J. V. Ortiz, Q. Cui, A. G. Baboul, S. Clifford, J. Cioslowski, B. B. Stefanov, G. Liu, A. Liashenko, P. Piskorz, I. Komaromi, R. L. Martin, D. J. Fox, T. Keith, M. A. Al-Laham, C. Y. Peng, A. Nanayakkara, M. Challacombe, P. M. W. Gill, B. Johnson, W. Chen, M. W. Wong, C. Gonzalez, J. A. Pople, *Gaussian 03*, Revision C.02, Gaussian, Inc., Wallingford CT, **2004**.
[27] J. L. J. Dearling, J. S. Lewis, D. W. McCarthy, M. J. Welch, P. J. Blower, *Chem. Commun.* **1998**, 2531.
[28] J. L. J. Dearling, J. S. Lewis, G. E. D. Mullen, M. J. Welch, P. J. Blower, *J. Biol. Inorg. Chem.* **2002**, *7*, 249.
[29] J. L. J. Dearling, P. J. Blower, *Chem. Commun.* **1998**, 2531.
[30] R. I. Maurer, P. J. Blower, J. R. Dilworth, C. A. Reynolds, Y. Zheng, G. E. D. Mullen, *J. Med. Chem.* **2002**, *45*, 1420.
[31] A. J. Bard, L. R. Faulkner, *Electrochemical Methods: Fundamentals and Applications*, 2nd ed., Wiley, New York, **2001**.
[32] J. P. Holland, J. C. Green, J. R. Dilworth, *Dalton Trans.* **2006**, 783.
[33] L. E. Warren, S. M. Horner, W. E. Hatfield, *J. Am. Chem. Soc.* **1972**, *94*, 6392.
[34] D. L. Maricle, W. G. Hodgson, *Anal. Chem.* **1965**, *37*, 1562.
[35] D. Vasudevan, H. Wendt, *J. Electroanal. Chem.* **1995**, *392*, 69.
[36] S. Stoll, A. Schweiger, *J. Magn. Reson.* **2006**, *178*, 42.
[37] Bruker, *Win-EPR SimFonia*, version 1.26 beta, http://www.bruker-biospin.com/simfonia.html.
[38] D. X. West, J. S. Ives, G. A. Bain, A. E. Liberta, J. Valdes-Martinez, K. H. Ebert, S. Hernandez-Ortega, *Polyhedron* **1997**, *16*, 1895.
[39] D. X. West, A. E. Liberta, S. B. Padhye, R. C. Chikate, P. B. Sonawane, A. S. Kumbhar, R. G. Yerande, *Coord. Chem. Rev.* **1993**, *123*, 49.
[40] D. X. West, S. B. Padhye, P. B. Sonawane, *Struct. Bonding (Berlin)* **1991**, *76*, 1.
[41] L. Tosi, A. Garnier-Suillerot, *J. Chem. Soc., Dalton Trans.* **1982**, 103.
[42] S. I. Gorelsky, *SWizard program*, Department of Chemistry, York University, Toronto, ON, Canada, **1998**, http://www.sgchem.net/.
[43] K. K. Irikura, R. D. Johnson III, R. N. Kacker, *J. Phys. Chem.* **2005**, *109*, 8430.
[44] A. R. Cowley, J. Davis, J. R. Dilworth, P. S. Donnelly, R. Dobson, A. Nightingale, J. M. Peach, B. Shore, D. Kerr, L. Seymour, *Chem. Commun.* **2005**, 845.
[45] A. Obata, E. Yoshimi, A. Waki, J. S. Lewis, N. Oyama, M. J. Welch, H. Saji, Y. Yonekura, Y. Fujibayashi, *Ann. Nucl. Med.* **2001**, *15*, 499.
[46] P. Hohenberg, W. Kohn, *Phys. Rev. B* **1964**, *136*, 864.
[47] W. Kohn, L. J. Sham, *Phys. Rev. B* **1965**, *140*, 1133.
[48] A. D. Becke, *Phys. Rev. A* **1988**, *38*, 3098.
[49] A. D. Becke, *J. Chem. Phys.* **1992**, *96*, 2155.
[50] A. D. Becke, *J. Chem. Phys.* **1992**, *97*, 9173.
[51] A. D. Becke, *J. Chem. Phys.* **1993**, *98*, 5648.
[52] S. H. Vosko, L. Wilk, M. Nusair, *Can. J. Phys.* **1980**, *58*, 1200.
[53] C. Lee, W. Yang, R. G. Parr, *Phys. Rev. B* **1988**, *37*, 785.
[54] R. Ditchfield, W. J. Hehre, J. A. Pople, *J. Chem. Phys.* **1971**, *54*, 724.
[55] W. J. Hehre, R. Ditchfield, J. A. Pople, *J. Chem. Phys.* **1972**, *56*, 2257.
[56] P. C. Hariharan, J. A. Pople, *Mol. Phys.* **1974**, *27*, 209.
[57] P. C. Hariharan, J. A. Pople, *Theor. Chim. Acta* **1973**, *28*, 213.
[58] M. M. Francl, W. J. Pietro, W. J. Hehre, J. S. Binkley, M. S. Gordon, D. J. DeFrees, J. A. Pople, *J. Chem. Phys.* **1982**, *77*, 3654.
[59] V. A. Rassolov, J. A. Pople, M. A. Ratner, T. L. Windus, *J. Chem. Phys.* **1998**, *109*, 1223.
[60] V. A. Rassolov, M. A. Ratner, J. A. Pople, P. C. Redfern, L. A. Curtiss, *J. Comput. Chem.* **2001**, *22*, 976.
[61] R. J. Hall, M. M. Davidson, N. A. Burton, I. H. Hillier, *J. Phys. Chem.* **1995**, *99*, 921.
[62] J. L. Chen, L. Noodleman, D. A. Case, D. Bashford, *J. Phys. Chem.* **1994**, *98*, 11059.
[63] J. Tomasi, B. Mennucci, R. Cammi, *Chem. Rev.* **2005**, *105*, 2999.
[64] M. L. Connolly, *Science* **1983**, *221*, 709.
[65] V. Barone, M. Cossi, J. Tomasi, *J. Chem. Phys.* **1997**, *107*, 3210.
[66] L. Y. Zhang, R. A. Friesner, *J. Phys. Chem.* **1995**, *99*, 16479.
[67] Z. Otwinowski, W. Minor, *Methods Enzymol.* **1997**, *276*, 307.
[68] A. Altomare, G. Cascarano, G. Giacovazzo, A. Guagliardi, M. C. Burla, G. Polidori, M. Camalli, *J. Appl. Crystallogr.* **1994**, *27*, 435.
[69] P. W. Betteridge, J. R. Carruthers, R. I. Cooper, K. Prout, D. J. Watkin, *J. Appl. Crystallogr.* **2003**, *36*, 1487.

Received: April 22, 2008
Published Online: June 24, 2008

